The Ammonia - Water Phase Diagram and its Implications for Icy Satellites

Mary L. Johnson and Malcolm Nicol

Department of Chemistry and Biochemistry, University of California, Los Angeles, CA 90024

Short Title: Ammonia - Water Phase Diagram

Abstract

We have used a Holzafpel-type diamond anvil cell to determine the NH_3 - H_2O phase diagram in the region from 0 to 33 mole percent NH_3, 240 to 370 K, and 0 to 5 GPa. The following phases were identified: liquid; water ices Ih, III, V, VI, VII, and VIII; ammonia monohydrate, $NH_3.H_2O$; and ammonia dihydrate $NH_3.2H_2O$. Ammonia dihydrate becomes prominent at moderate pressures (less than 1 GPa), with planetologically significant implications, including the possibility of layering in Titan's magma ocean.

Introduction

The geology and history of icy bodies in the solar system can only be understood if the phase relations of their constituent ices are known. The principal ice-forming component molecules in the solar system are water (H_2O), methane (CH_4), and ammonia (NH_3). These compounds are expected to occur in the solar system abundance ratios for O, C, and N: 100 to 25 to 18 [Hunten, et al., 1983]. As water ice is the predominant solid ice phase, methane and ammonia are most likely to be stable as hydrates: methane as methane clathrate hydrate ($CH_4.6H_2O$) and ammonia as ammonia dihydrate ($NH_3.2H_2O$) or monohydrate ($NH_3.H_2O$). While the properties of icy bodies with core pressures of less than 0.5 GPa (such as Enceladus and Mimas) can be predicted based on atmospheric-pressure phase diagrams, understanding the larger and more tectonically active icy satellites such as Titan and Triton require knowledge of phase relations to at least 5 GPa.

The effect of ammonia on ice phases is potentially much greater than that of methane, since ammonia and water form stoichiometric compounds with properties distinctly different from those of water ices. The lack of data on the stability of ammonia hydrates at planetologically important pressures has prompted our study of the NH_3-H_2O phase diagram to 5 GPa.

We have based our work on a number of previous

studies: especially important are the investigations of the NH_3-H_2O system at atmospheric pressure by Clifford and Hunter [1933] and Rollet and Vuillard [1956]. The rheology of ammonia-water liquids under pressure has been studied by McKinnon and Meadows [1984]. The P-T phase diagram for H_2O has been determined by several investigators; we take the work of Mishima and Endo [1980] as a starting point. The ammonia P-T phase diagram has been investigated by Mills and coworkers [Mills et al., 1982], and we have previously described the P-T melting curve for ammonia monohydrate [Johnson et al., 1985].

For the purposes of this investigation, we have chosen to examine only the pressure range relevant to icy satellites, 0 to 5 GPa; the temperature range relevant to the high-pressure liquidus surface, 240 to 370 K; and the composition range relevant to the water-ice/ammonia hydrate eutectic, 0 to 33 mole percent NH_3. Preliminary results have been communicated in Johnson et al. [1983, 1984, and 1985] and in Johnson and Nicol [1985].

Experimental

Starting Materials and Operating Conditions

Compounds below 31 mole percent NH_3 were made from mixtures of concentrated reagent aqueous ammonia and distilled water, without further purification or degassing. Compositions were checked in two ways: either by titration, with an accuracy of 0.1 mole percent NH_3; or by density measurements at known temperatures, back-calibrated to titrated standards, with an estimated accuracy of 0.2 mole percent NH_3. For compounds with greater than 31 mole percent ammonia, samples were made from gaseous ammonia (99.99% pure) and distilled water, mixed by weight in a stainless steel loading line, and loaded under pressure. Sample compositions were checked *a posteriori* by dilution and titration.

Each sample was mounted in a hardened 316 stainless steel gasket in a diamond anvil cell (DAC) of the Holzapfel type [Hirsch and Holzapfel, 1981], which allowed fine adjustment of pressure in the pressure range we examined. The pressure was monitored by using the ruby luminescence technique [Piermarini *et al.*, 1975]. Liquids with high ammonia concentrations were introduced into the DAC in a 316 stainless steel loading box.

The phases present in each sample were determined by visual inspection, usually in plane-polarized light. For variable-temperature runs, the DAC was mounted in a

cryostat with fused quartz windows, connected to a circulating bath filled with water-antifreeze mixture and heated by 50-watt resistors. Some of the room temperature runs and all of the variable temperature runs were observed with rotating crossed polarizers in place; this simplified the identification of many phases.

Identification of Phases

The following phases were routinely seen in the DAC: Ices VI, VII, and VIII; ammonia monohydrate, $NH_3.H_2O$; and ammonia dihydrate, $NH_3.2H_2O$. Ices Ih, III, and V were rarely seen. Each of the ammonia compounds appeared to have one structure over the range of pressures and temperatures we observed.

Ice VII resembled its description in the literature [Whatley and Van Valkenburg, 1967; Yamamoto, 1980]. Ice VI was usually seen as a rime-like frosting on the diamond surface, with low polarization colors. Blocky crystals matching the description of Ice VI by Yamamoto [1982] were identified as Ice V and only seen in its stability field; the Ice V crystals had much higher polarization colors than Ice VI. Ice VIII looked just like Ice VII, but was stable over a different temperature range; during the transition between Ice VII and Ice VIII, boundaries between grains developed high relief, then disappeared entirely. Ice III was tentatively identified as the cloudy solid seen at low temperatures. In one set of runs, Ice Ih was also seen; this looked frostlike, much

like Ice VI.

Ammonia monohydrate was only seen (with Ice VII or VIII) as a product of the breakdown of ammonia dihydrate at high pressures. High pressure monohydrate is nearly isotropic and has a medium high relief, higher than that of dihydrate and less than that of Ices VII and VIII. Under oblique illumination it is tinted blue. The properties of high-pressure monohydrate are consistent with the structure reported for orthorhombic ammonia monohydrate at low temperature and ambient pressure [Olovsson and Templeton, 1959].

Ammonia dihydrate has a very low relief, comparable to that of the more water-rich liquid accompanying it in these investigations. Crystals were strongly polarized and usually twinned, polysynthetically or in cross-like twins with arms at 70°. The crystals cracked along the polysynthetic twin planes as pressure was applied: these are therefore cleavage planes as well. Between crossed polarizers, dihydrate was often seen to have two extinctions at 70° because of the twinning. At room temperature, dihydrate has the same relief as 15 mole percent ammonia solution and was only visible with crossed polarizers. The dihydrate phase seen in our investigation may have the same structure as its low temperature counterpart, which is known from powder diffraction data [Bertie and Shehata, 1984].

Liquid was observed as isotropic material with relief similar to that of dihydrate and subhedral (concave)

boundaries. On the time scale of our experiments, crystals persisted long after their first melting was observed; melting was identified by the dissolution of crystal boundaries.

Because the sample in the DAC is small and inaccessible to prodding, we sometimes experienced difficulty in nucleating phases, especially Ice VI. In order to overcome this difficulty, we lowered the pressure to the bottom of the Ice VI stability field where nucleation was enhanced. Metastable melting was a similar problem: Ice VII, for instance, would melt rather than form the more stable Ice VI as pressure decreased. Because of this, for all points in Tables 1 and 2, we have noted the direction in P-T space from which the sample has evolved; presumed metastable states are labelled with the letter "μ".

Greek "mu" →

Results - the Phase Diagram

Table 1 lists the phases seen for NH_3-H_2O mixtures at various pressures and room temperature. Table 2 gives the phases seen in variable temperature (cryostat) runs. All non-metastable points at 294±2 K are plotted in Figure 1. This is slightly different from previous versions of this figure [Johnson *et al*. 1983, 1984, 1985] and consistent with the total data set. The entire data set in P-T space is shown in Figures 2a through 2i, which are sections at constant bulk composition. A consistent set of phase boundaries is also indicated on these diagrams.

The liquidus is shown as a P-x projection contoured for temperature in Figure 3, and the P-T projection of the phase diagram as a whole is shown in Figure 4. Specific details of the phase diagram are discussed below.

Water Ice Relations

To the limit of precision of this study, none of the boundaries between solid phases of water are shifted by the presence of ammonia. Therefore, to first order, the activity of NH_3 in Ices VI, VII, and VIII is zero. Of course, increasing the amount of ammonia present increases the stability of the liquid relative to ice, thus supressing the ice melting curves.

Ice - Dihydrate - Liquid Eutectic

At room temperature, the Ice VI - dihydrate - liquid

eutectic is at 17 mole percent ammonia and 1.58 GPa. From atmospheric pressure to 2.0 GPa, the Ice (any phase) - dihydrate - liquid eutectic curve can be fit by the equation:

$$T_{eu} = 174 + 112.5\ P_{eu} - 22.9\ P_{eu}^2 \quad (r = 0.83)$$

where the curve has been fit through the dihydrate melting point at atmospheric pressure (174 K), as well as through our data. The eutectic curve is well fit by the expression

$$x_{eu} = 13.35 + 2.52\ P_{eu} \quad (r = 0.96)$$

in the range 0.7 to 2.0 GPa (240 to 300 K); x_{eu} should curve back toward dihydrate composition both as pressure approaches one atmosphere and above 2 GPa (see Figure 3).

Dihydrate Melting Curve

At room temperature, dihydrate melts at 0.88 GPa. Assuming there is only one dihydrate phase between atmospheric pressure and 3.4 GPa, the pure dihydrate melting curve can be approximated as a polynomial in ln P:

$$T_m = 296.1 + 17.5 \ln P_m + 0.47 (\ln P_m)^2$$

where T_m is in K and P_m in GPa. This curve is a better fit to the melting data than one that is either quadratic

in P or linear in (ln P).

Dihydrate Decomposition at Pressure

Dihydrate breaks down to Ice VII (or Ice VIII) plus monohydrate at 3.45 GPa; this result is apparently independent of temperature. The monohydrate plus Ice VII mixture remains stable at room temperature to at least 14.7 GPa.

The Higher Ammonia Region

Points with greater than 33 mole percent NH_3 are reported in Figure 2i. This region is currently being explored by other workers (S. Boone, UCLA, pers. comm., 1986) and will not be discussed further here.

Monohydrate Phase Relations

Melting of monohydrate was seen in the 5 mole percent NH_3 sample at 3.87 GPa and a temperature somewhere above 313 K. The value of 330 K has been adopted for this melting point from comparison with similar amounts of laser heating in pure H_2O runs. This value is also consistent with the monohydrate melting curve (Figure 5).

Discussion - the Phase Diagram

The main result of this study is the discovery that ammonia dihydrate should be a major rock-forming (ice-forming) compound in the interiors of icy satellites; this was not anticipated because of the small dihydrate stability range at low pressure. Dihydrate does not condense from nebular gases, but will form from liquid at depths as shallow as 1 km (0.02 GPa) for Titan-sized satellites.

The melting curve of dihydrate has been approximated as a polynomial in (ln P). This description of dihydrate melting behavior suggests that the compressibility difference between dihydrate and melt along the melting curve is not constant but decreases monotonically with increasing pressure, which may be due to continuous changes in the structure of the melt. (Similar behavior is seen in the melting of the alkali metals [Zha and Boehler, 1985], an analogy that may be more misleading than useful.)

The anomalous melting properties and unexpectedly low relief of dihydrate would make more sense if this phase were itself a glass. Glass is commonly formed instead of crystalline phases in the freezing of ammonia-water mixtures at low pressure [Rollet and Vuillard, 1956, Van Kasteren, 1973]. However, the dihydrate phase is unlikely to be a glass for a simple reason: it is strongly anisotropic, as seen from its polarization colors. (Even

dihydrate in contact with liquid is strongly polarized, so stress alone does not explain this.)

We have assumed that our high-pressure dihydrate is the same phase as ambient pressure dihydrate. The implications of this assumption for planetary modelling are discussed by Lunine and Stevenson [1986]. This idea could be tested by optical examination of the low-pressure phase, and by crystal structure determination of high-pressure dihydrate. The extent of compositional variation in dihydrate at high pressures can be determined by point counting and quantitative refractive index determination, and by further synthesis experiments.

In summary, it is important to emphasize the features of this research of which we are most certain: the enhanced stability of dihydrate with pressure; its physical properties (density, twinning, cleavage) and optical anisotropy; and especially the pressure, temperature and compositional dependence of the water ice-dihydrate melting surface between 240 and 320 K.

Planetary Implications

Previous calculations by planetary modellers [Lewis, 1971; Consolmagno, 1975, 1983, 1985; Hunten et al., 1983] have included ammonia as monohydrate or as the atmospheric-pressure eutectic liquid, which has a composition close to that of ammonia dihydrate. For understanding accretion and processes on the surfaces of icy satellites, this approach is probably sufficient. Recognition of the existence of dihydrate leads to a new understanding of the fate of ammonia at depth, however, and of its effect on processes at depth. Lunine [1985] and Lunine and Stevenson [1985, 1986] have included dihydrate in their thermal models of satellite evolution; but for physical and tectonic models, the following properties of dihydrate may also be relevant:

i. Ammonia dihydrate forms in significant amounts only from a melt under pressure, monohydrate being the phase that condenses from a vapor or at low pressure.

ii. Dihydrate neither sinks below nor floats above the eutectic liquid at 1.5 GPa pressure; a similar, more stable balance is expected to occur at much lower pressure.

iii. Owing to the fracture/cleavage/twinning planes seen in dihydrate, large single crystals should have zones of weakness where sliding would be enhanced.

The second point will be further elucidated in an example based on a model from Lunine and Stevenson.

The magma ocean and atmosphere of Titan

Lunine and Stevenson [1986] present a model for Titan's evolution in which, for a long period in the satellite's development, a methane-depleted water/ammonia ocean is present, capped by Ice I and underlain by water ice, clathrates, and rock. As the ocean cools, phases crystallize, the first being water ice, which, depending on the pressure at which it is formed, will either float to the top (Ice Ih) or sink to the ocean floor (other ice phases).

Over a limited pressure range (see Figure 4), dihydrate will crystallize first. Whether it is more or less bouyant than the accompanying liquid depends on the composition of the liquid and on the pressure and temperature of crystallization, since dihydrate is comparable to 15% ammonia solution in density. At a point where the density of dihydrate is equal to that of the melt, the stability of a dihydrate layer depends on the relative curvature of the pure dihydrate melting curve and of the eutectic curve in P-T space (Figure 5). At high pressure (1.7 GPa), dP/dT is greater for dihydrate melting than for eutectic melting, so dihydrate will gradually float or sink away from a point where the two have equal density. At low pressures however (T < 200 K), since the eutectic becomes less ammonia-rich (denser) as pressure increases, dP/dT is less for dihydrate than for eutectic melt, and dihydrate crystals can segregate into a distinct

layer, which might be preserved as the magma cools. Obviously, convection in the magma ocean would tend to break up this layer.

Summary

We have demonstrated that ammonia dihydrate has significantly enhanced stability at high pressures and controls the ammonia-water eutectic melt at the cosmic ammonia/water composition. The addition of ammonia to the chemical basis for modelling icy planets can lead to unexpected properties for the surfaces and interiors of these bodies and to modified evolutionary schemes. This work demonstrates the importance of pressure as a variable in planetary petrology, and illustrates the usefulness of the diamond anvil cell as a gateway to the high pressure regime.

Acknowledgments

The experimental portion of this investigation was much facilitated by Andrea Schwake Koumvakalis, Steve Boone, Ahziz Karem, June Yen, and Susanna Johnson, UCLA; and both theory and practice were much improved by discussions with Reinhard Boehler. Our interpretations were greatly clarified by interactions with Dave Stevenson, Jon Lunine, and Mark Parisi. We thank Guy Consolmagno for calling previous work to our attention, and we give joyful thanks to NASA for their long-suffering support (Grant NAGW-104). The California Space Institute also provided funding.

References

Bertie, J. E. and M. R. Shehata, Ammonia dihydrate: preparation, x-ray powder diffraction pattern and infrared spectrum of $NH_3.2H_2O$ at 100 K, J. Chem. Phys., 81, 27-30, 1984.

Clifford, I. L. and E. Hunter, The system ammonia-water at temperatures up to 150°C and at pressures up to twenty atmospheres, J. Chem. Phys., 37, 101-118, 1933.

Consolmagno, G. J., Thermal history models of icy satellites, M. S. thesis, Massachusetts Institute of Technology, 1975.

Consolmagno, G. J., Ice-rich moons and the physical properties of ice, J. Phys. Chem., 87, 4204-4208, 1983.

Consolmagno, G. J., Resurfacing Saturn's satellites: models of partial differentiation and expansion, Icarus, 64, 401-413, 1985.

Hirsch, K. R. and W. B. Holzapfel, Diamond anvil high pressure cell for Raman spectroscopy, Rev. Sci. Instruments, 52, 52-55, 1981.

Hunten, D. M., M. G. Tomasko, F. M. Flasar, R. E.

Samuelson, D. F. Strobel, and D. J. Stevenson, Titan, in Saturn, edited by T. Gehrels and M. S. Matthews, pp. 671-787, University of Arizona Press, Tucson, 1984.

Johnson, M. L. and M. Nicol, The ammonia - water phase diagram II: extent and significance of ammonia dihydrate, $NH_3.2H_2O$ (abstract), EOS, Trans. AGU, 66, 944, 1985.

Johnson, M. L., M. Nicol, and A. Schwake, Preliminary phase diagram for the water-rich region of the system NH_3 - H_2O to 4.0 GPa (abstract), EOS, Trans. AGU, 64, 875, 1983.

Johnson, M. L., A. Schwake, and M. Nicol, The ammonia - water phase diagram I: water-rich region at low (<4 GPa) pressure (abstract), Fifteenth Lunar and Planetary Science Conference Abstracts, p. 405-406, Lunar and Planetary Science Institute, Houston, 1984.

Johnson, M. L., A. Schwake, and M. Nicol, Partial phase diagram for the system NH_3 - H_2O: the water-rich region, in Ices in the Solar System, edited by J. Klinger et al., p. 39-47, D. Reidel, Amsterdam, 1985.

Lewis, J. S., Satellites of the outer planets: thermal models, Science, 172, 1127, 1971.

Lunine, J. I., Volatiles in the outer solar system, Ph.D.

thesis, 326pp., California Institute of Technology, 1985.

Lunine, J. I. and D. J. Stevenson, Thermodynamics of clathrate hydrate at low and high pressures with application to the outer solar system, Astrophys. J. Suppl., 58, 493-531, 1985.

Lunine, J. I. and D. J. Stevenson, Clathrate and ammonia hydrates at high pressure: application to the origin of methane on Titan, Icarus, submitted, 1986.

McKinnon, W. B. and M. Meadows, Rheological measurements of ammonia-water melt (abstract), Bull. Am. Astr. Soc., 16, 686, 1984.

Mills, R. L., D. H. Liebenberg, and Ph. Pruzan, Phase diagram and transition properties of condensed ammonia to 10 kbar, J. Phys. Chem., 86, 5219-5222, 1982.

Mishima, O. and S. Endo, Phase relations of ice under pressure, J. Chem. Phys., 73, 2454-2456, 1980.

Olovsson, I. and D. H. Templeton, The crystal structure of ammonia monohydrate, Acta Cryst., 12, 827-832, 1959.

Piermarini, G. J., S. Block, J. D. Barnett, and R. A. Forman, Calibration of the pressure dependence of the R1 ruby fluorescence line to 195 kbar, J. Appl. Phys., 46,

2774-2780, 1975.

Rollet, A.-P. and G. Vuillard, Sur un nouvel hydrate de l'ammoniac, Comtes. rendus Acad. Sci. Paris, 243, 383-386, 1956.

Van Kasteren, P. H. G., The crystallization behavior and caloric properties of water-ammonia mixtures between 70 K and 300 K, Bull. Inst. Int. Froid. Annexe, 4, 81-87, 1973.

Whatley, L. S. and A. Van Valkenberg, High pressure optics, in Advances in High Pressure Research, edited by R. S. Bradley, p. 327-371, Academic Press, London, 1967.

Yamamoto, K., Supercooling of the coexisting states of ice VII and water within the ice VI region observed in diamond-anvil pressure cells, Jap. J. Appl. Phys., 19, 1841-1845, 1980.

Yamamoto, K., A morphological observation of ice VI, Jap. J. Appl. Phys., 21, 803, 1982.

Zha, C.-S. and R. Boehler, Melting of sodium and potassium in a diamond anvil cell, Phys. Rev., B31, 3199-3201, 1985.

Authors' Addresses:

Mary L. Johnson

Division of Geological and Planetary Sciences

170-25

California Institute of Technology

Pasadena, CA 91104

Malcolm Nicol

Department of Chemistry and Biochemistry

University of California

Los Angeles, CA 90024

Figure Captions

Fig. 1. Isothermal 294±2 K phase diagram for the water-rich region of the NH_3-H_2O system. The coding for points is explained in Figure 2j. Abbreviations: D - Ammonia dihydrate, $NH_3.2H_2O$; M - Ammonia monohydrate, $NH_3.H_2O$; L - Liquid; VI - Ice VI; VII - Ice VII.

Fig. 2. Pressure-temperature phase diagram for the water-rich region of the NH_3 - H_2O system, sectioned by mole percent NH_3. Pure H_2O tie-lines are shown as reference lines on all figures. (a) 0% NH_3. (b) Phase boundaries drawn for 5% NH_3. (c) Boundaries drawn for 10% NH_3. (d) Boundaries drawn for 13% NH_3. (e) Boundaries drawn for 15% NH_3. (f) Boundaries drawn for 20% NH_3. (g) Boundaries drawn for 25% NH_3. (h) Boundaries drawn for 30% NH_3. (i) Phase boundaries drawn for pure dihydrate, 33.3% NH_3. (j) Legend.

Fig. 3. Liquidus contoured at indicated temperatures, P - x projection. Abbreviations: L - Liquid; D - Dihydrate; M - Monohydrate; Ih - Ice Ih; Roman numerals - Water Ices.

Fig. 4. Water-rich region of the NH_3 - H_2O phase diagram, P - T projection, contoured in mole percent NH_3. Where dihydrate is the liquidus phase, lines are solid; where a water ice is the liquidus phase, lines are dotted.

Fig. 5. Dihydrate and monohydrate melting curves and the water ice-dihydrate eutectic between 175 and 325 K. The numbers refer to mole percent NH_3 at the eutectic composition.

Table 1. Room temperature runs.

Composition mole % NH_3 ±0.2	P GPa ±0.03	T K ±1	Direction of Approach	Phases Present
0.0	2.52	296	P↓	7
	2.70	296	P↓	7
	1.80	293	P↓	μ(7+L)
	0.98	293	P↓	μL
	1.23	293	P↑	μL
	2.38	293	P↑	7
	2.18	293	P↑↑	7
	2.13	293	P↓	7
	2.21	293	P↓	7
	1.95	293	P↓	μ(7+L)
4.7	1.13	292	P↑	6
	1.11	292	P↓	6+L
	0.31	292	P↓	L
	2.14	292	P↑	7
	2.03	292	P↓	6
	2.36	292	P↑	7
	1.74	292	P↓	6
	1.07	292	P↓	6+L
	1.34	292	P↑	6+L
	0.99	292	P↓	L
10.3	2.25	292	P↑	7+D
	2.13	292	P↓	7
	1.73	292	P↓	L
	1.58	292	P↑	L

10.3	1.97	292	P↓	μL
13.5	2.21	295	P↓	7+L
	3.79	295	P↓	7+M
	3.37	295	P↓	7+D
	2.85	295	P↓	7+D
	1.57	295	P↓	L
19.2	3.97[a]	293	P↓	7
	1.47[a]	293	P↓	D+L
	2.51[a]	293	P↓	7+D
	2.23[a]	293	P↓	D
	1.50[a]	293	P↓	L
	2.44[a]	293	P↓	7
	2.22[a]	293	P↓	7+D
	2.82[a]	296	—	D
	1.76	296	P↓↓	μL
	3.06	296	P↓	7+D
	1.31	296	P↓	L
	2.01	296	P↓↓	D
	1.93	296	P↓	D
	1.54	296	P↓	L
	0.16	296	P↓	L
24.3	1.79	292	P↓	D+L
	2.00	292	P↓	μ(D+L)
	1.10	292	P↓	D+L
	1.22	292	P↓	D+L
	2.13	292	P↓	D
	1.93	292	P↓	6+D

24.3	3.35	292	P↑	7+D
	3.40	292	—	7+D
31.1	1.65	294	P↑	D
	1.68	294	P↓	D+L
	1.71	294	P↓	D+L
	1.86	294	P↓	D+L
	1.74	294	P↓	D+L
	1.13	294	P↓	D
	0.02	294	P↓	L

Notes to Table 1:

Phases: 7 - Ice VII; 6 - Ice VI; L - liquid; D - ammonia dihydrate; M - ammonia monohydrate. μ indicates a metastable assemblage (see text).

[a] These points are ±0.07 GPa.

Table 2. Pressure-Temperature runs.

Composition mole % NH_3 ±0.1	P GPa ±0.03	T K ±1	Direction of Approach	Phases Present
0.0	1.04	290	P↑	6
	1.06	313	T↑	6
	1.43	333	T↑	6
	1.40	352	T↑	L
	1.40	372	T↑	L
	0.99	250	T↓	μL
	2.06	250	P↑	8
	2.44	267	T↑	8
	2.36	271	T↑	8
	3.01	293	T↑	7
	3.07	312	T↑	7
	3.37	333	T↑	7
	4.61	250	P↑T↓	8
	3.30	251	P↓	8
	1.89	252	P↓	8
	2.17	257	T↑	6+8
	2.14	262	T↑	6
	2.09	267	T↑	6
	0.28	293	T↑	L
	0.44	293	—	L
	0.29	263	T↓	L
	0.32	253	T↓	μL
	0.36	249	T↓	3
	0.33	254	T↑	3

0.0	2.03	293	T↑P↑	6
	1.81	294	—	6
	1.88	302	T↑	6
	1.84	310	T↑	6
	1.79	294	T↑	6
	1.68	312	T↑	6
	1.78	317	T↑	6+L
	1.92	321	T↑	6+L
5.0	3.90	293	P↑	7
	3.87	328[a]	T↑	7+L
	4.12	277	T↑	7+M
	4.20	263	T↑	8+M
	4.50	245	T↑	8+M
	3.32	247	P↑	8+D
	3.10	249	T↑	8+D
	2.99	261	T↑	8+D
	2.50	267	T↑	8+D
	2.43	270	T↑	8+D
	2.25	274	T↑	7+D
	2.03	276	T↑	μ(7+D)
	2.29	284	P↑T↑	7+D
	2.04	292	T↑	μ(7+D)
	1.96	298	T↑	μ(7+D)
	2.09	298	T↑	7+D+L
	1.91	301	T↑	μ(7+L)
	2.01	295	T↑	7
	1.77	288	T↑P↑	6

5.0	1.88	282	T↓	6
10.7	4.78	291	P↓	7+M
	4.21	291	P↓	7+M
	3.98	292	P↓	7+M
	4.20	292	P↓	7+M
	4.12	292	P↓	7+M
	3.74	292	P↓	7+M
	3.67	292	P↓	7+M
	3.58	293	—	7+M
	3.53	293	P↓	7+M
	3.18	293	P↓	7+D
	2.12	293	P↓	6+D
	2.64	293	—	7+D
	1.74	290	P↓	μ(7+L)
	1.91	252	T↓	8+D
	2.01	246	T↓	8+D
	1.49	245	T↓	6+D
	1.49	248	T↓	6+D
	1.48	253	T↓	6+D
	1.52	257	T↓	6+D
	1.48	262	T↓	D+L
	1.48	267	T↓	L
	1.46	271	T↓	L
	1.54	275	T↓	L
	1.62	280	T↓	L
	1.76	283	T↓	L
	1.66	245	T↓	6+D

10.7	1.80	245	P↓	6+D
	1.41	245	P↓	6+D
	1.48	245	T↓	6+D
	1.50	253	T↓	6+L
	1.38	258	T↓	6+L
	1.29	262	T↓	6+L
	1.27	266	T↓	6+L
	1.32	271	T↓	6+L
	1.21	276	T↓	6+L
	0.82	246	T↓	6+L
	0.85	247	T↓	6+L
	0.90	249	T↓	6+L
	0.95	254	T↓	L
	0.95	258	T↓	L
	0.96	261	T↓	L
	1.12	265	T↓	L
	1.11	269	T↓	L
	1.11	273	T↓	L
	1.11	276	T↓	L
	1.14	280	T↓	L
	1.78	262	T↓↓	6+D+L
	1.77	268	T↓	6+L
	1.67	272	T↓	6+L
	1.84	276	T↓	L
	1.97	283	T↓	L
	2.04	286	T↓	L
	1.94	288	T↓	L

10.7	1.87	292	T↑	L
	1.76	297	T↑	L
12.9	2.92	290	P↑	7+D
	2.50	290	P↓	7+D
	2.34	264	T↓	8+D
	2.50	253	T↓	8+D
	2.46	254	T↑	8+D
	2.50	259	T↑	8+D
	2.45	264	T↑	8+D
	2.53	267	T↑	8+D
	2.54	246	T↓	8+D
	1.08	246	P↓	6+D
	0.98	248	T↑	6+D+L
	0.68	249	P↓	5+L
	0.60	249	—	5+L
	0.56	248	—	5+L
	0.58	245	T↓	5+L
	0.68	245	P↑	5+6+D
	0.68	246	—	6+D
	0.79	248	T↑	6+L
	0.79	249	T↑	L
	1.01	249	P↑T↓	6+D
	1.06	253	T↑	6+D
	1.02	257	T↑	6+D
	1.11	261	T↑	6+D
	1.12	267	T↑	6+D
	1.08	272	T↑	6+D

12.9	1.17	276	T↑	L
	1.24	281	T↑	L
	0.60	293	T↑	L
	0.57	294	—	L
15.0	1.95	290	P↑	6+D
	2.05	292	T↑	6+D
	2.12	293	T↑	6+D
	2.11	295	T↑	6+D+L
	2.10	298	T↑	L
	2.06	307	T↑	L
	1.83	316	T↑	L
	1.96	307	—	D+L
	2.01	306	P↑	D+6
	2.55	299	P↑T↓	7+D
	2.50	301	T↑	7+D+L
	2.49	306	T↑	7+L
	2.50	313	T↑	7+L
	2.40	314	T↑	7+L
	2.50	315	T↑	7+L
	2.58	318	T↑	L
	2.45	322	T↑	L
	2.53	327	T↑	L
	2.65	334	T↑	L
	2.05	292	T↓	7+D
	1.73	292	P↓	D+L
	1.70	285	T↓	D+6
	1.56	271	T↓	6+D

15.0	1.63	258	T↓	6+D
	0.41	249	P↓T↓	μ(6+D)
	0.03	248	—	1+L
	0.02	249	T↓	1+L
	0.23	254	T↓	L
	0.13	259	T↓	L
	0.17	263	T↓	L
	0.32	268	T↓	L
	0.35	276	T↓	L
20.0	2.78	294	P↓	7+D
	3.09	294	P↓	7+D
	2.94	294	P↓	7+D
	2.76	294	P↓	7+D
	2.85	297	T↓	7+D
	2.78	302	T↓	7+D
	2.86	312	T↓	D+L
	2.78	333	T↓	L
	1.70	293	T↓P↓↓↓	6+D
	1.77	294	T↓	6+D+L
	1.74	300	T↓	D+L
	1.75	306	T↓	L
	1.78	313	T↓	L
	1.92	326	T↓	L
	2.43	341	T↓	L
	2.35	342	—	L
	1.44	292	T↓	μL
	2.04	292	P↓↓	6+D

20.0	1.97	292	P↓	6+D
	2.08	292	P↓	6+D
	1.97	292	P↓	6+D
	0.37	293	P↓	L
	0.63	252	T↓	6+D
	0.42	248	T↓	6+D
	0.28	249	T↑	D+L
	0.48	253	T↑	L
	0.59	259	T↑	L
	0.64	263	T↑	L
	0.79	268	T↑	L
	0.71	273	T↑	L
	0.71	278	T↑	L
	0.99	283	T↑	L
	1.18	287	T↑	L
	1.14	289	T↑	L
	0.27	248	T↓	D+L
	0.43	248	—	D+L
	0.17	250	T↑	L
	0.39	253	T↑	L
	0.32	258	T↑	L
	0.46	264	T↑	L
	0.48	268	T↑	L
	0.53	273	T↑	L
	0.82	277	T↑	L
	1.04	286	T↑	L
	0.89	290	T↑	L

25.0	4.64	294	P↓	7+M
	4.24	293	P↓	7+M
	3.87	293	P↓	7+M
	3.31	293	P↓	7+M
	3.32	293	P↓	7+M
	3.21	293	—	7+D
	2.21	293	P↓	7+D
	2.41	293	P↓	7+D
	2.02	292	—	7+D
	1.66	294	T↓	D+L
	1.82	298	T↓	D+L
	1.83	304	T↓	D+L
	1.97	307	T↓	L
	1.94	312	T↓	L
	1.87	321	T↓	L
	1.72	330	T↓	L
	1.74	330	T↓	L
	1.08	336	T↓	L
	1.24	347	T↓	L
	0.85	349	P↓	L
	0.40	348	P↓	L
	14.66	291	P↓	7+M
	1.77	291	P↓	D
	1.70	291	—	D
	1.10	291	P↓	D
	1.16	291	—	D
	1.17	291	—	D

25.0	1.91	294	T↑	D
	1.68	300	T↑	D
	1.54	304	T↑	D
	1.41	308	T↑	D+L
	1.40	313	T↑	L
	1.38	318	T↑	L
	1.29	322	T↑	L
	1.07	327	T↑	L
	1.14	332	T↑	L
	1.05	335	T↑	L
	1.60	293	T↓	D
	1.26	303	P↓T↑	L
	1.24	307	T↑	L
	0.89	308	—	L
33.2	2.18	295	T↓	μL
	2.64	251	P↑T↓P↓	D
	2.67	250	T↑	D
	2.46	272	T↑	D
	2.09	292	P↓	L
34.0	3.81	292	P↑	7+M
	3.58	296	—	7+M
	3.73	296	P↓	7+M
	3.54	296	P↓	7+M
	2.86	296	P↓	μ(7+M)
	2.48	296	P↓	D
	2.60	293	—	D
	2.53	296	T↑	D

34.0	2.55	299	T↑	D
	2.54	303	T↑	D
	1.89	242	T↓	D
	2.44	242	P↑	D
	2.45	268	T↑	D
	2.43	278	T↑	D
	2.51	286	T↑	D
	2.48	297	T↑	D
	2.47	305	T↑	L
	2.53	313	T↑	L
	2.66	325	T↑	L
	2.62	341	T↑	L
	2.73	343	T↑	L
	2.71	356	T↑	L
	2.58	356	P↓	L
	2.67	355	P↓	L
	2.72	355	—	L

Notes to Table 2:

Phases: 1 - Ice Ih; 3 - Ice III; 5 - Ice V; 6 - Ice VI; 7 - Ice VII; 8 - Ice VIII; D - ammonia dihydrate; M - ammonia monohydrate; L - liquid. μ indicates a metastable assemblage (see text).

[a] Temperature approximate; see discussion in text.

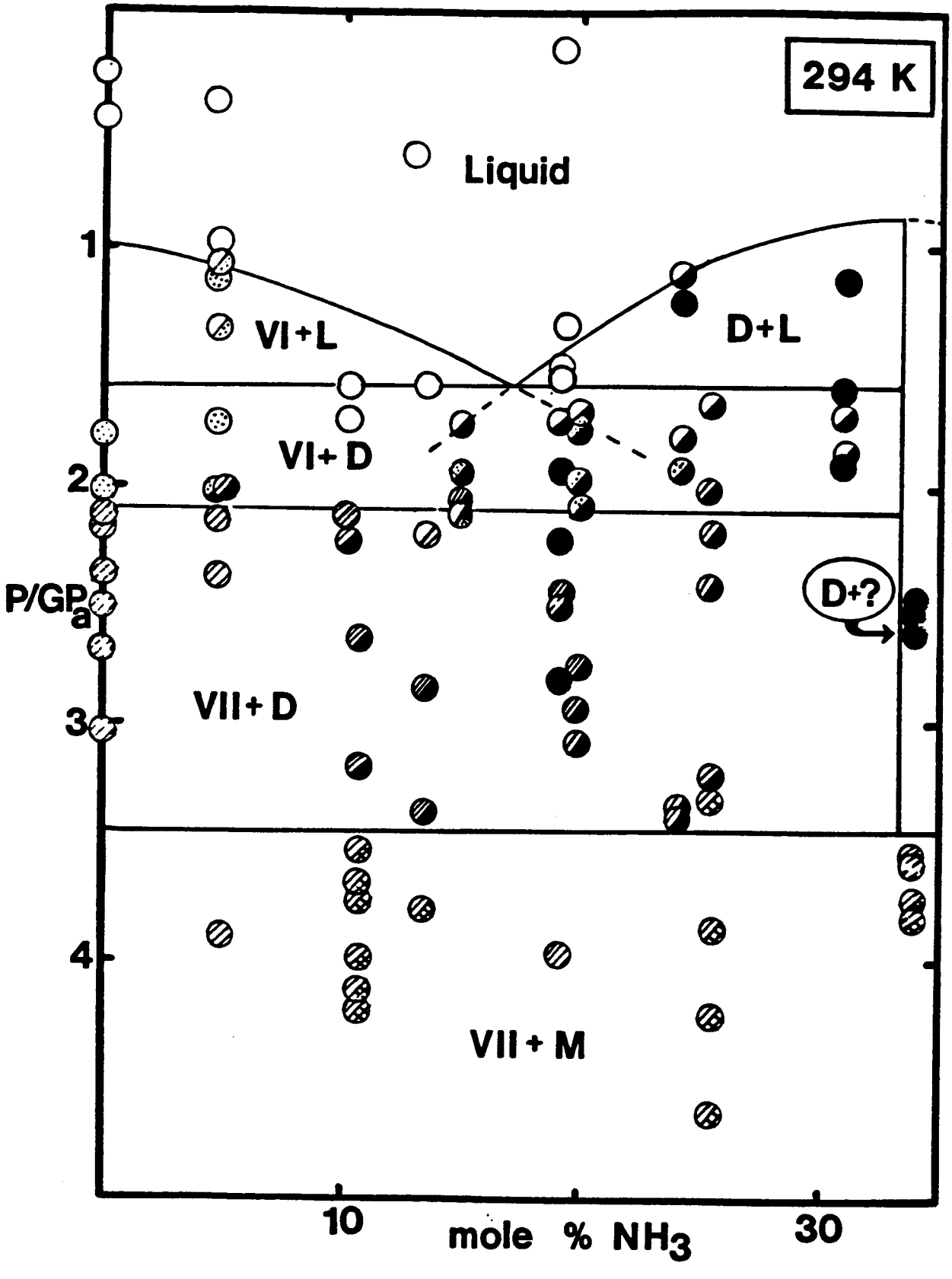
294 K
Liquid
VI+L
D+L
VI+D
D+?
VII+D
VII+M
1
2
3
4
P/GPa
10
mole % NH3
30

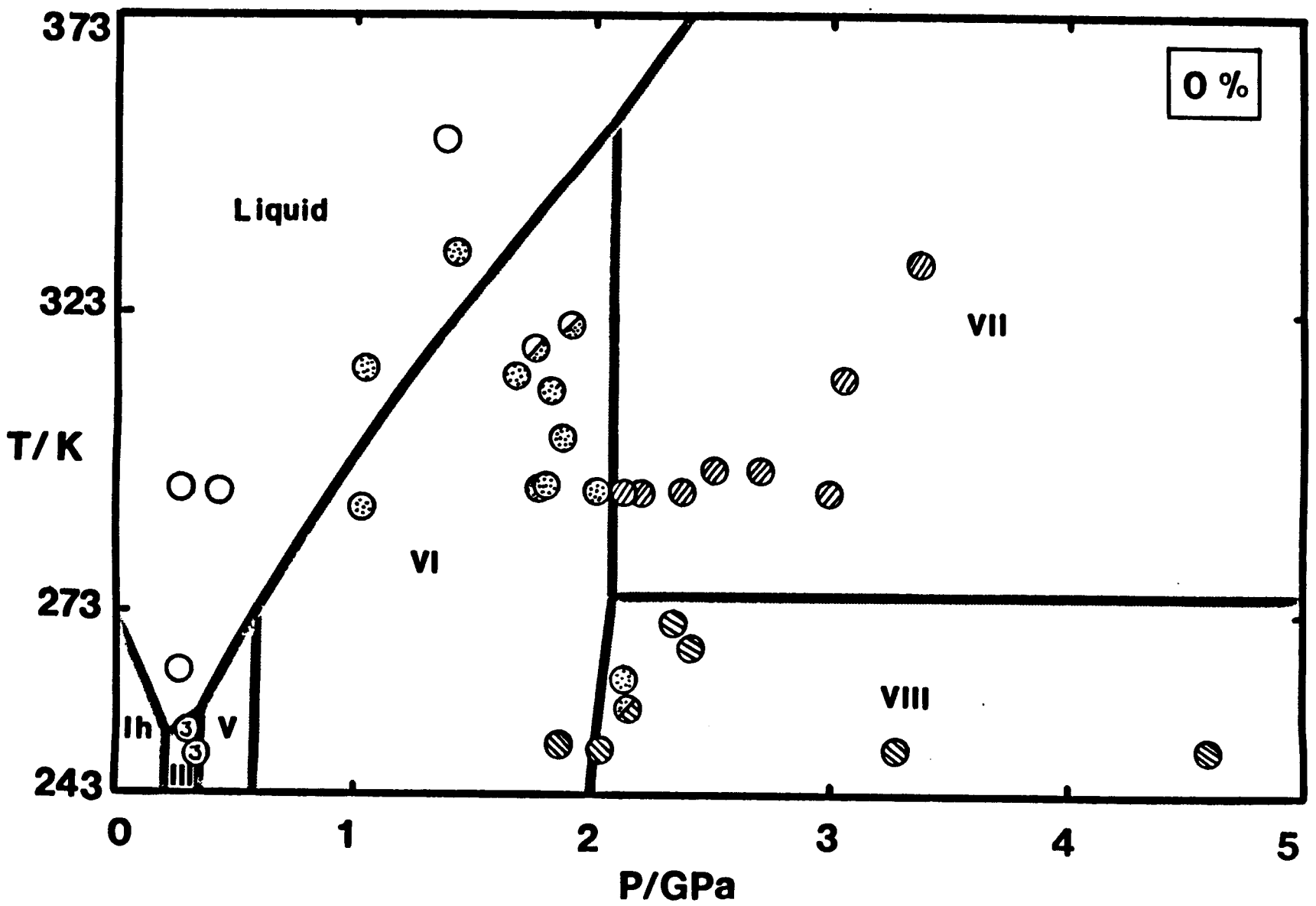
373
323
273
243
T/K
0 %
Liquid
VI
VII
VIII
Ih
V
III
0
1
2
3
4
5
P/GPa

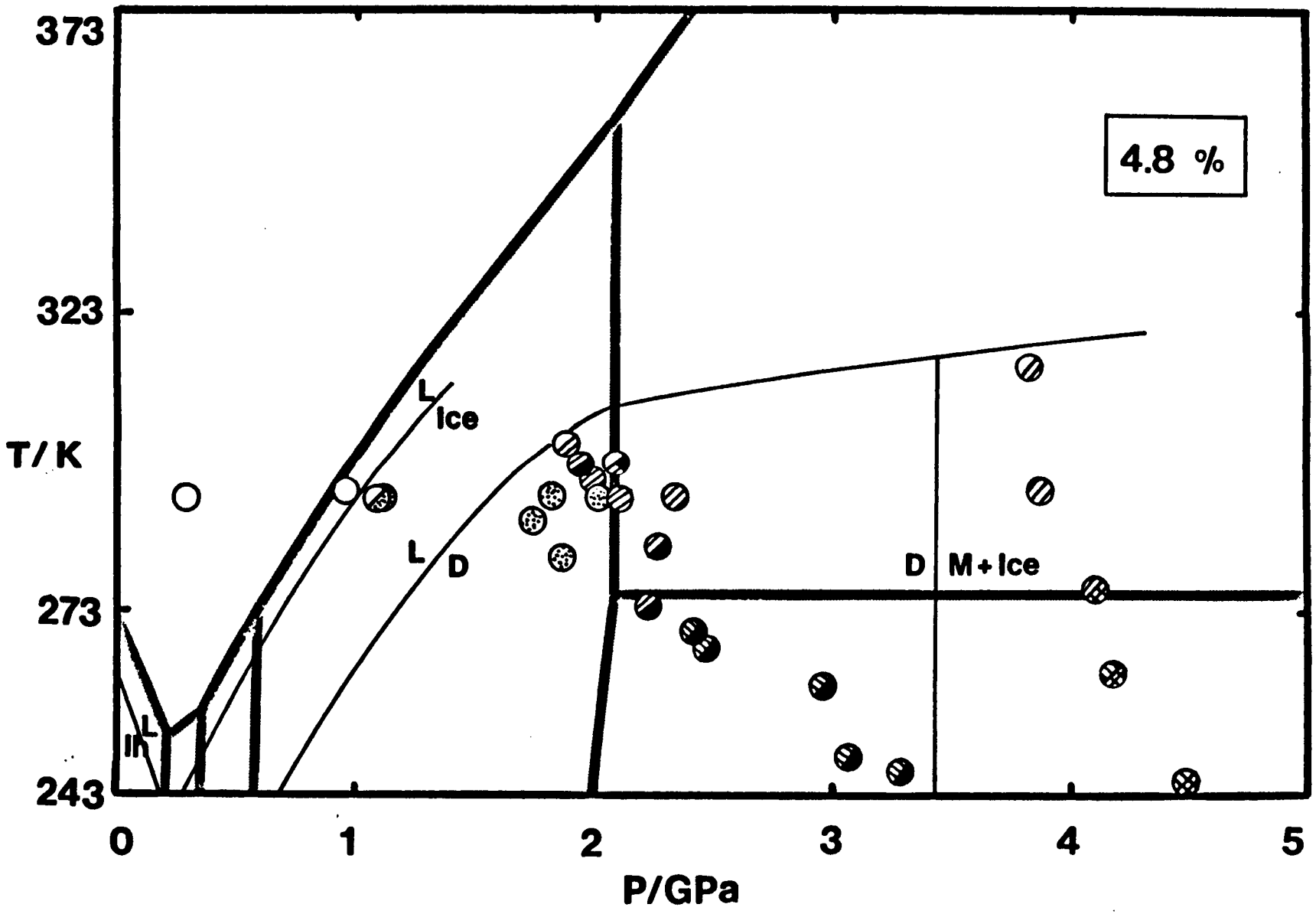
373
323
273
243
T/K
0
1
2
3
4
5
P/GPa
4.8 %
L
Ice
L
D
D
M+Ice
II
L

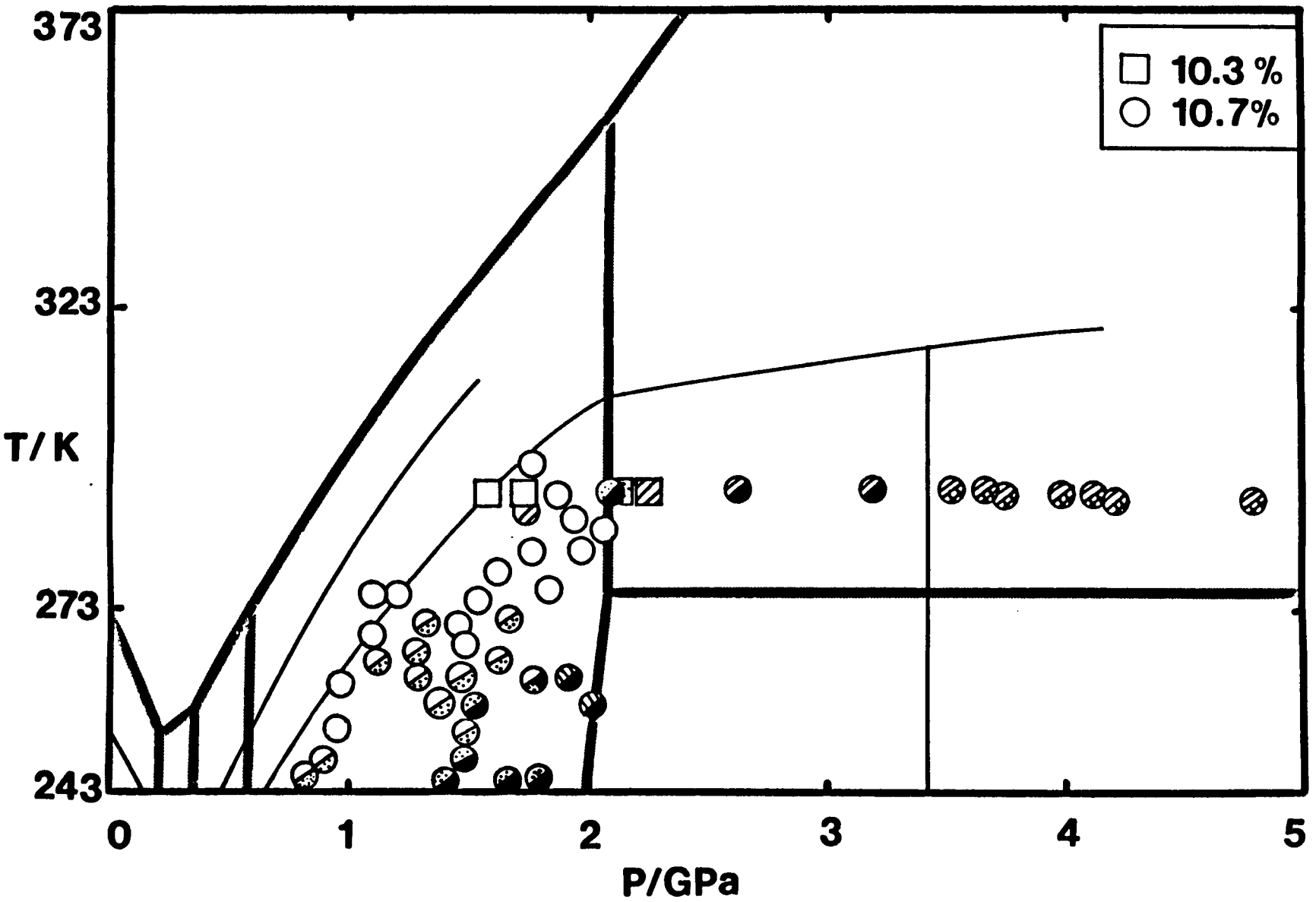
373
323
273
243
T/K
0
1
2
3
4
5
P/GPa
10.3 %
10.7%

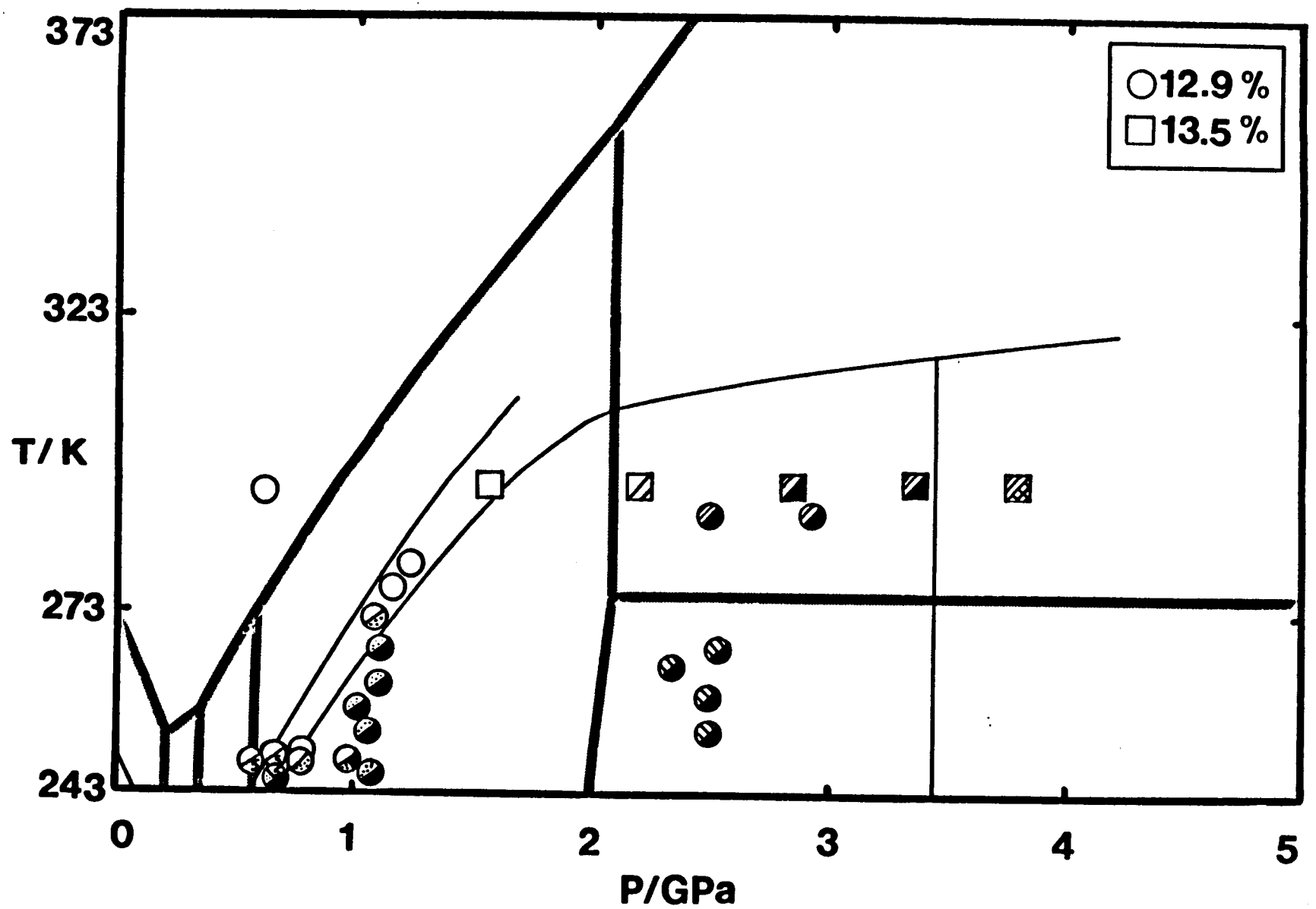
373
323
273
243
T/K
0
1
2
3
4
5
P/GPa
○12.9 %
□13.5 %

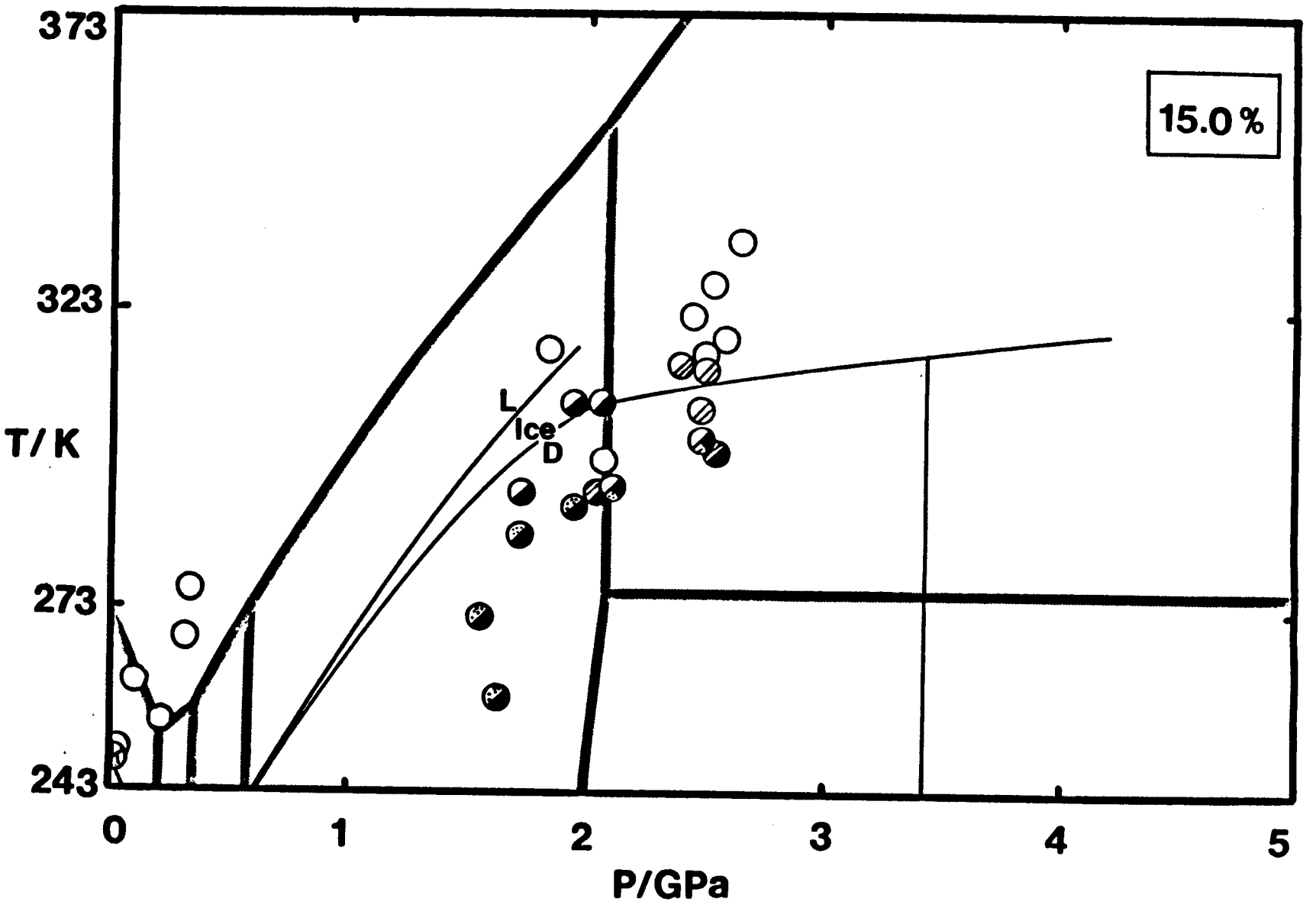
373
323
273
243
T/K
0
1
2
3
4
5
P/GPa
15.0 %
L
Ice
D

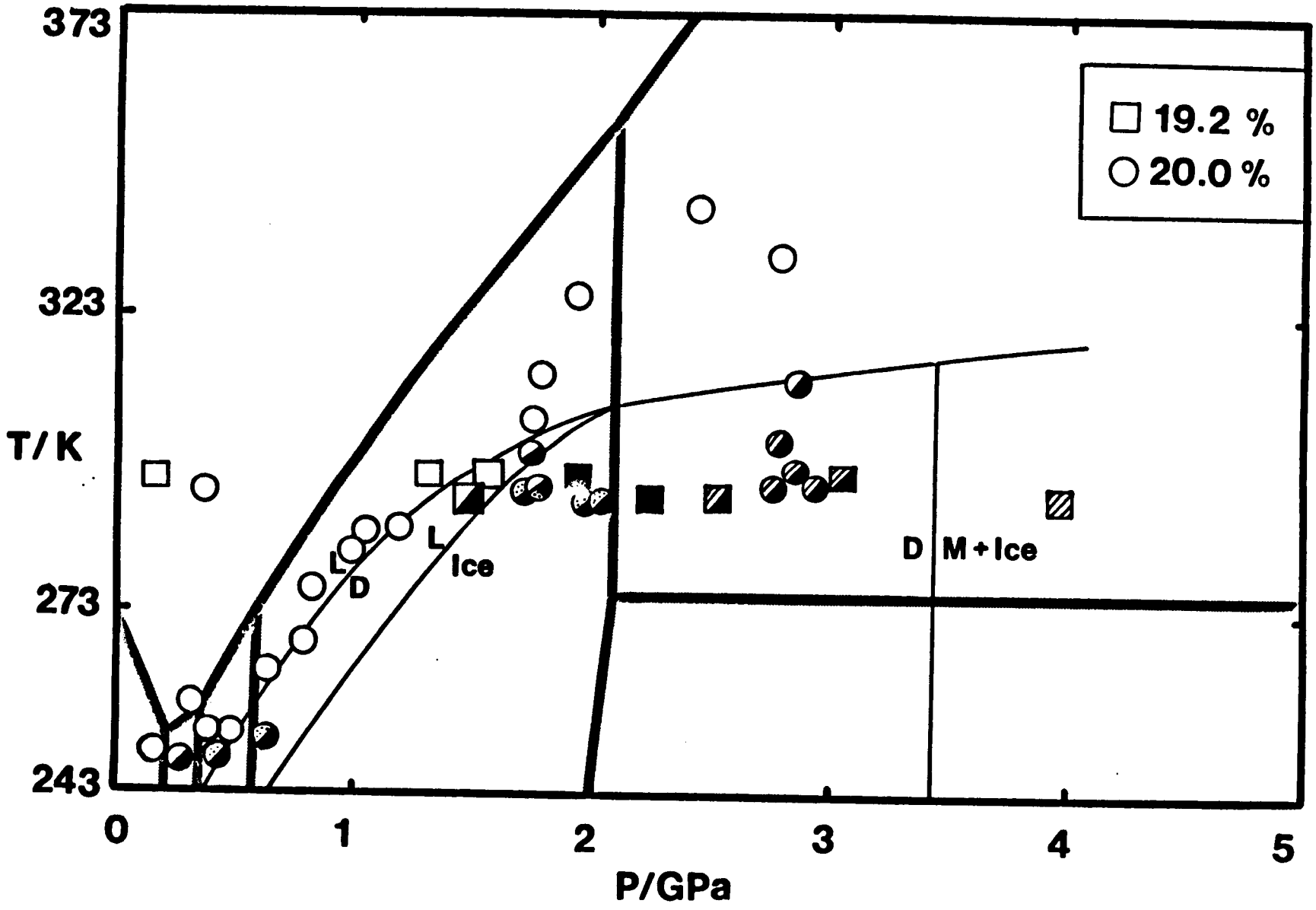
373
323
273
243
T/K
0
1
2
3
4
5
P/GPa
19.2 %
20.0 %
L
D
L
Ice
D
M + Ice

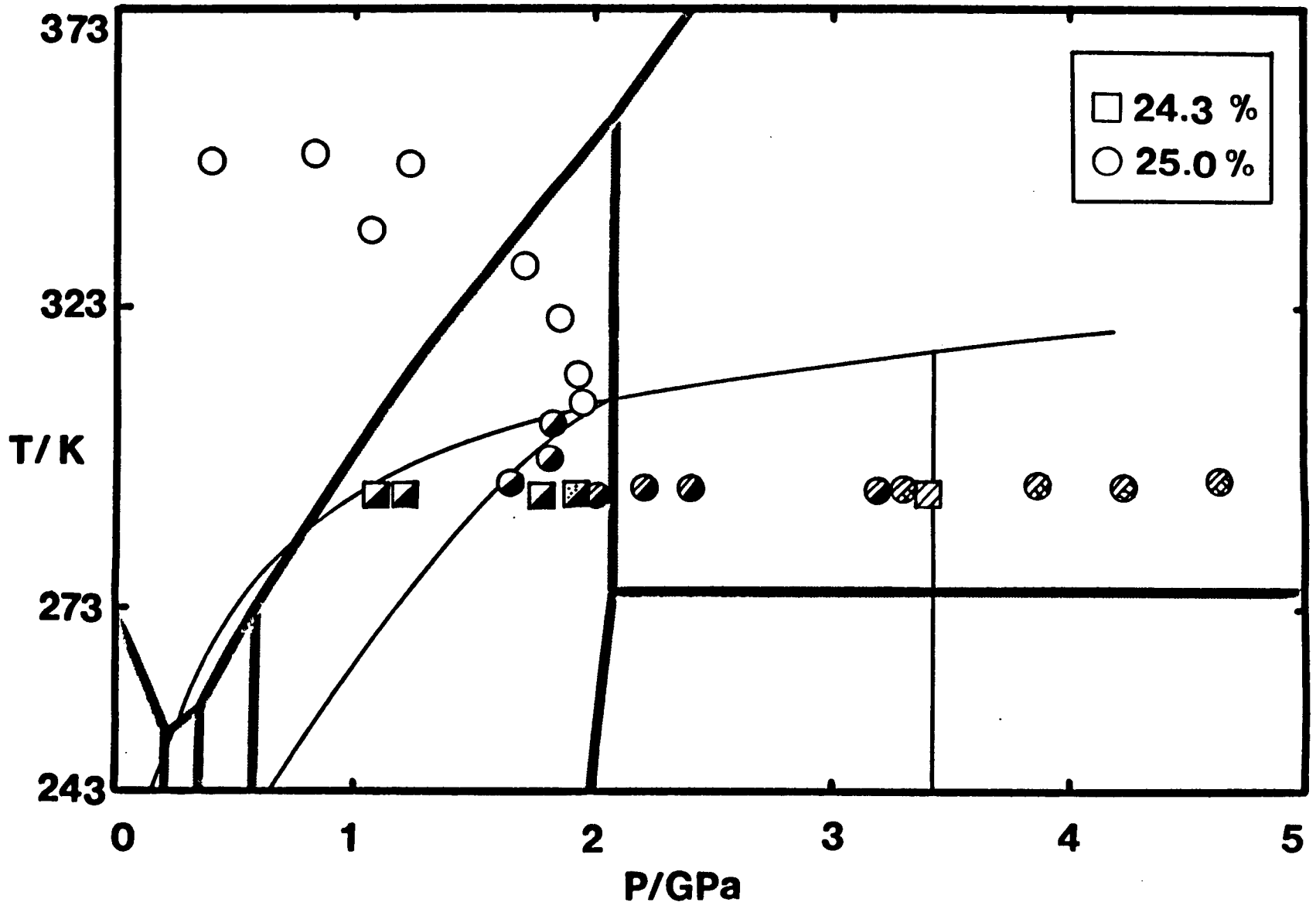
373
323
273
243
T/K
0
1
2
3
4
5
P/GPa
24.3 %
25.0 %

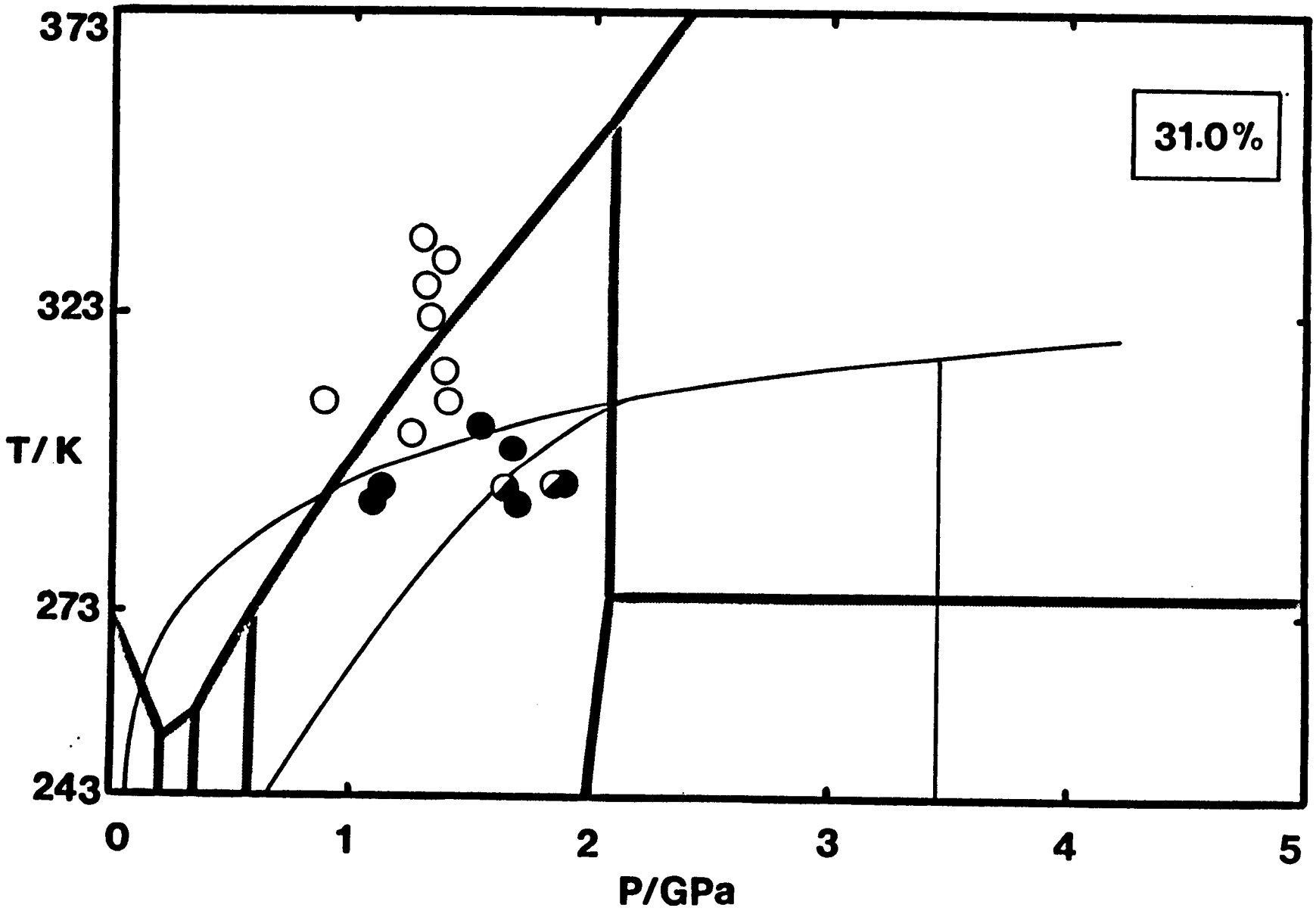
373
323
273
243
T/K
0
1
2
3
4
5
P/GPa
31.0%

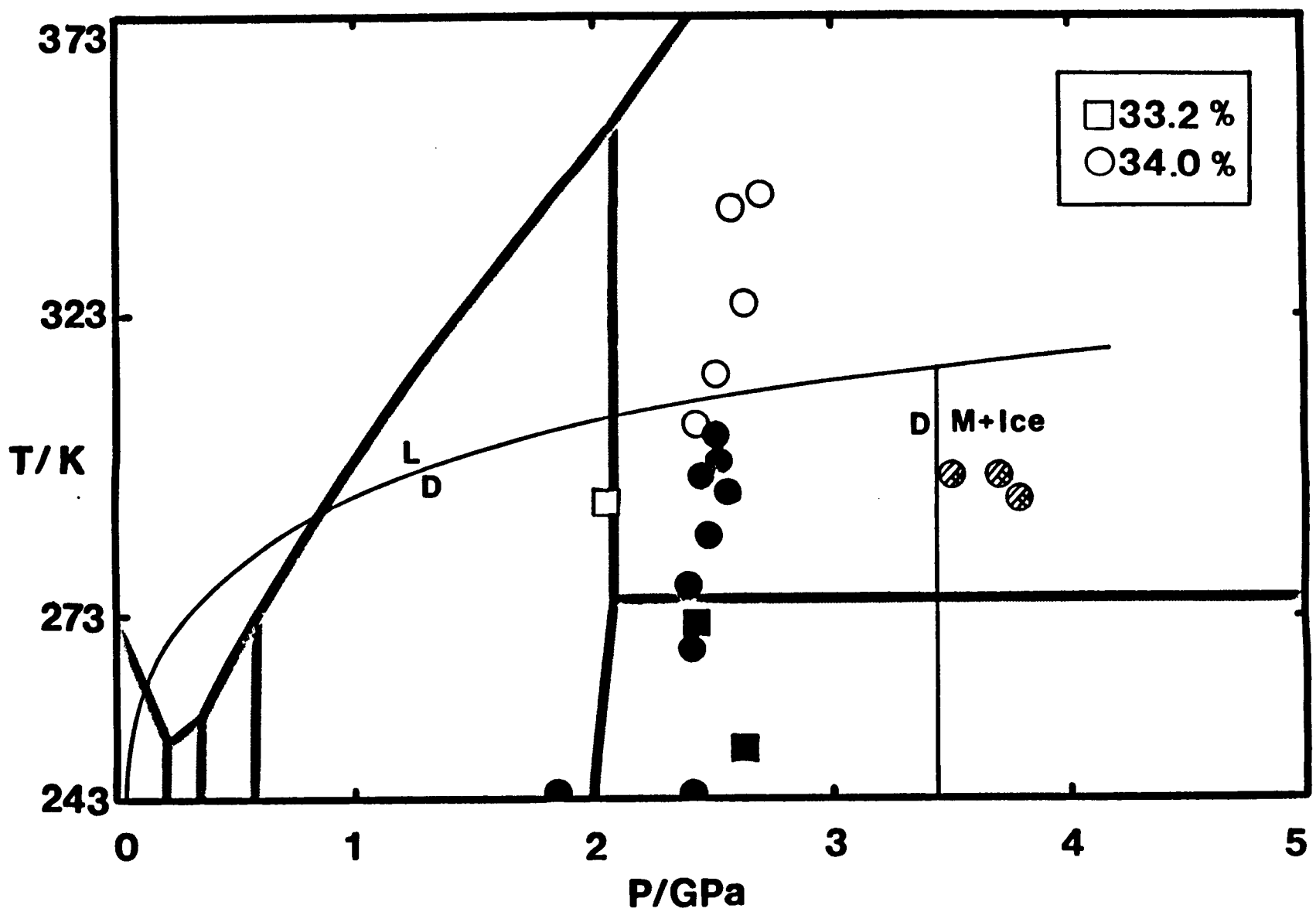
373
323
273
243
T/K
0
1
2
3
4
5
P/GPa
33.2 %
34.0 %
L
D
D
M+Ice

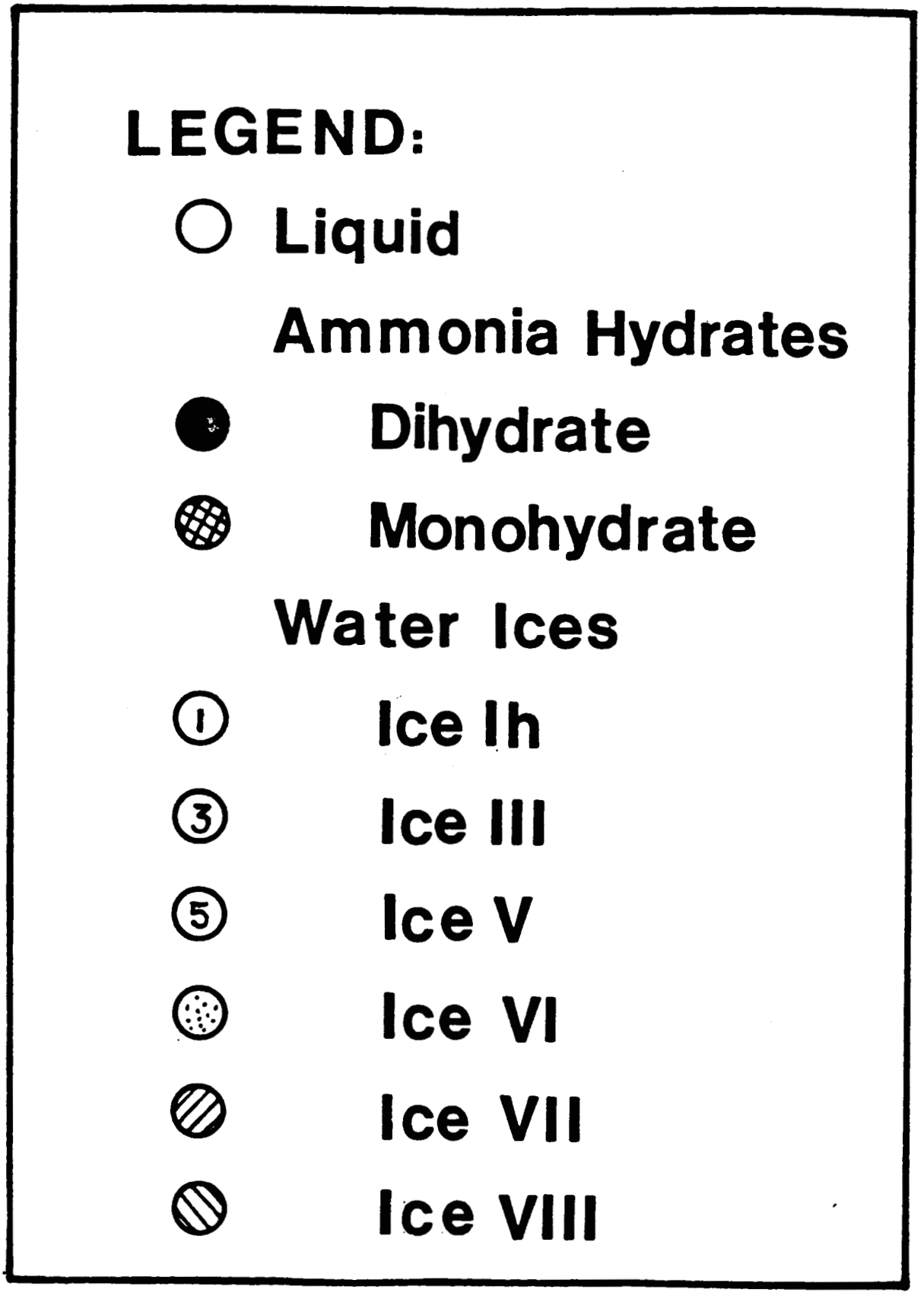
LEGEND:
Liquid
Ammonia Hydrates
Dihydrate
Monohydrate
Water Ices
Ice Ih
Ice III
Ice V
Ice VI
Ice VII
Ice VIII

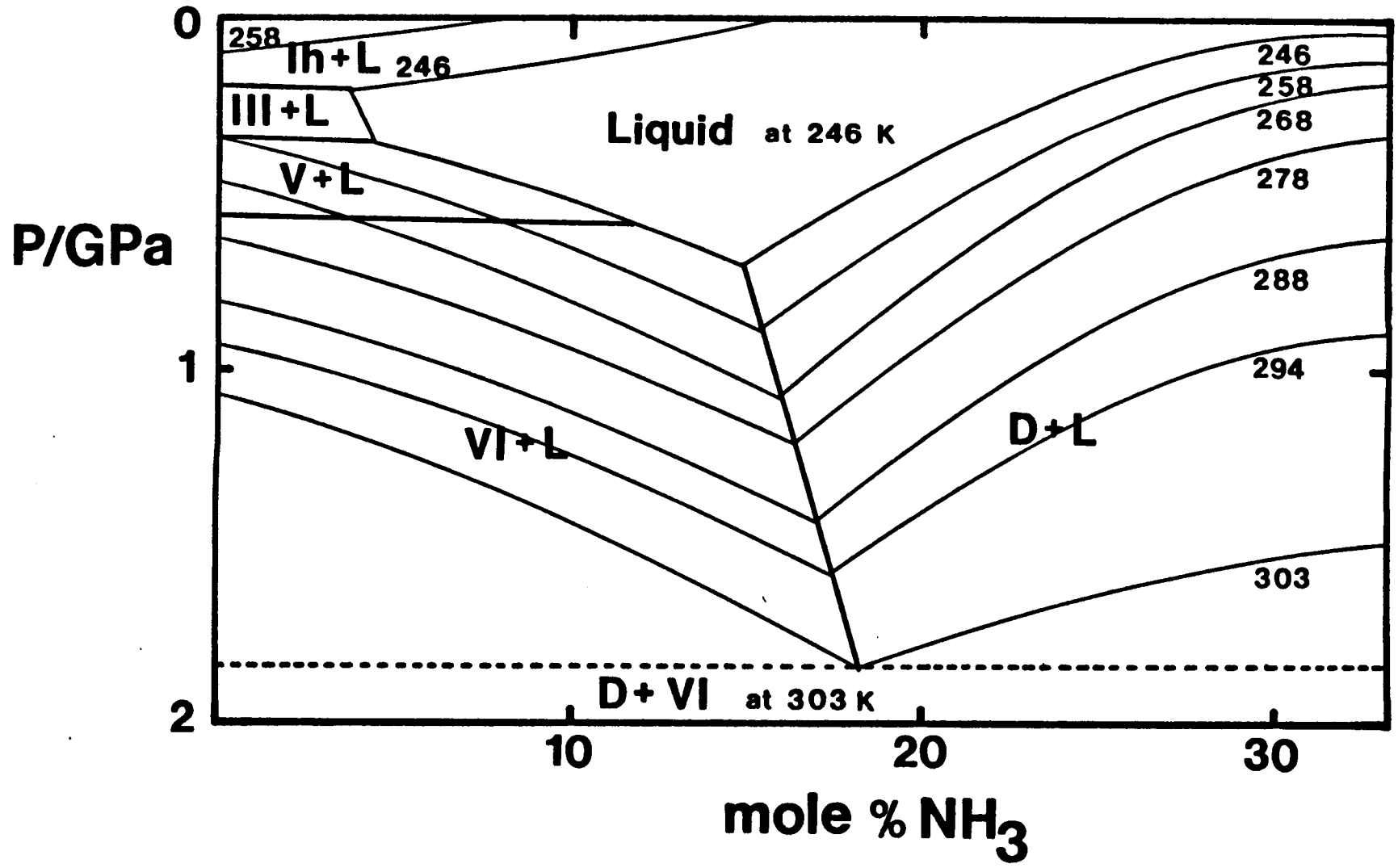
0
1
2
P/GPa
258
Ih+L 246
III+L
V+L
Liquid at 246 K
VI+L
D+L
D+VI at 303 K
246
258
268
278
288
294
303
10
20
30
mole % NH3

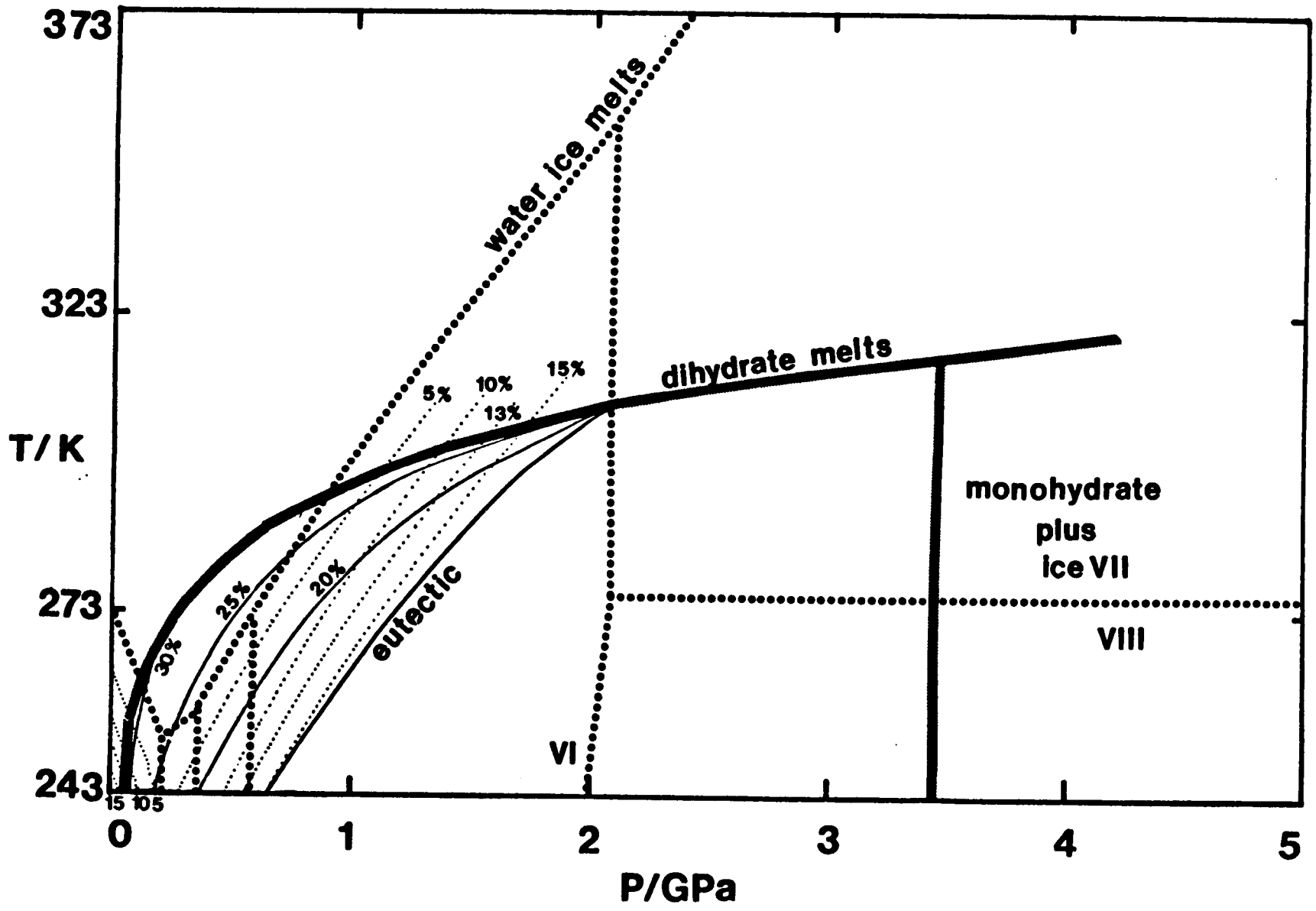
373
323
273
243
T/K
water ice melts
dihydrate melts
5%
10%
13%
15%
20%
25%
30%
eutectic
VI
monohydrate
plus
ice VII
VIII
15
105
0
1
2
3
4
5
P/GPa

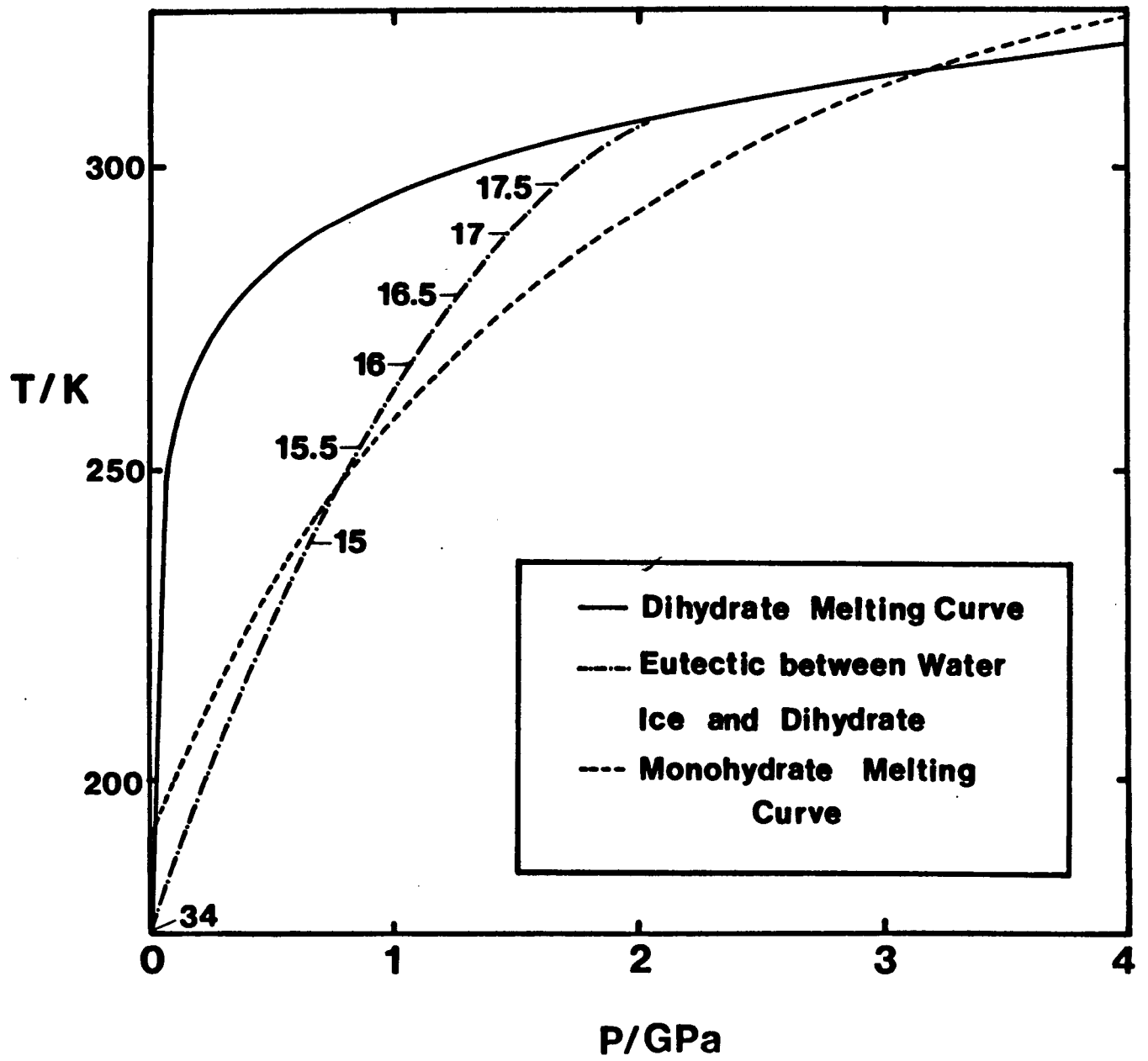
300
250
200
T/K
17.5
17
16.5
16
15.5
15
34
0
1
2
3
4
P/GPa
Dihydrate Melting Curve
Eutectic between Water Ice and Dihydrate
Monohydrate Melting Curve